Shell Effects in Neutron Capture on Pb

T. Rauscher*, R. Bieber†, S. Lingner†, H. Oberhummer†

*Institut für Kernchemie, Universität Mainz, Germany
†Institut für Kernphysik, Technische Universität, Vienna, Austria

We calculate direct neutron capture on $^{210-228}$Pb with energy levels and masses taken from two different models. A sharp drop in the cross sections due to the lack of low spin states is seen with RMFT levels but cannot be found with the folded-Yukawa shell model.

I. INTRODUCTION

Over the last years it has been realized that the direct reaction mechanism cannot only dominate the reaction cross sections involving light elements. Also for intermediate and heavy nuclei it can become important near shell closures or for neutron rich isotopes when the level density becomes too low for the compound nucleus mechanism. Recently, we calculated direct capture (DC) cross sections for a number of cases (1,2). In this work we want to focus on (n,γ) reactions on the even-even isotopes $^{210-228}$Pb. They are of importance in the r-process path going to very heavy elements.

II. DIRECT CAPTURE AND FOLDING PROCEDURE

The theoretical cross section $\sigma^{\rm th}$ is derived from the DC cross section $\sigma^{\rm DC}$ given by (3)

$$\sigma^{\rm th} = \sum_i C_i^2 S_i \sigma_i^{\rm DC} \quad . \tag{1}$$

The sum extends over all possible final states (ground state and excited states) in the residual nucleus. The isospin Clebsch-Gordan coefficients and spectroscopic factors are denoted by C_i and S_i, respectively. The DC cross sections $\sigma_i^{\rm DC}$ are essentially determined by the overlap of the scattering wave function in the entrance channel, the bound-state wave function in the exit channel, and the multipole transition operator. For the computation of the DC cross section we used the direct capture code TEDCA (4).

For determining the nucleon-nucleus potential the folding procedure was employed, a method already successfully applied in the description of many systems. In this approach the nuclear target density $\rho_{\rm T}$ (derived from experimental charge distributions or from theory) is folded with an energy and density dependent nucleon-nucleon interaction $v_{\rm eff}$ (5):

© 1993 American Institute of Physics

$$V(R) = \lambda V_{\rm F}(R) = \lambda \int \rho_{\rm T}(\vec{r}) v_{\rm eff}(E, \rho_T, |\vec{R} - \vec{r}|) d\vec{r} \quad , \tag{2}$$

with $\vec{R}$ being the separation of the centers of mass of the two colliding nuclei. The normalization factor λ accounts for effects of antisymmetrization and is close to unity. The potential obtained in this way ensures the correct behavior of the wave functions in the nuclear exterior. At the low energies considered in astrophysical events the imaginary parts of the optical potentials are small.

III. ENERGY LEVELS AND MASSES

The levels (and masses) needed as input for the DC calculation were taken from two different approaches. The first one was the relativistic mean field theory (RMFT) which has turned out to be a successful tool for the description of many nuclear properties (6). The RMFT describes the nucleus as a system of Dirac nucleons interacting via various meson fields. There are six parameters which are usually obtained by fits to finite nuclear properties. For our calculations we have used the parameter set NLSH (7,8). Also the density distributions needed for the determination of the folding potentials were derived from RMFT wave functions.

The second method is the shell model developed by Möller et al. (9). In this model folded-Yukawa potentials are used in the determination of the single-particle potentials. For pairing the Lipkin-Nogami pairing model (10) is employed. This shell model proved to be very successful in reproducing ground state spins along magic numbers (11) and has been used in QRPA calculations of β-decay half lives (11) and as microscopic part in nuclear mass determinations (12).

To be able to compare the predictions from both models the nuclei were considered to be spherically symmetric.

IV. RESULTS AND DISCUSSION

Having obtained the relevant spins and Q-values (masses) as discussed above we still had to determine the strength parameter λ of the scattering potentials (see Equation (2)). This was done by adjusting λ so that experimental scattering data for ^{208}Pb+n at low energies were reproduced. In the potentials for each of the other isotopes a factor λ was chosen giving the same volume integral as for the fitted ^{208}Pb-potential. For the bound state potentials λ is fixed by the requirement of correct reproduction of the binding energies. The spectroscopic factors were assumed to be unity for all transitions considered.

The results of our calculations are summarized in Fig. 1. The most striking feature is the sudden drop over several orders of magnitude in the cross sections calculated with the RMFT levels. This is due to the lack of low spin levels which are cut off by the decreasing neutron separation energy. For

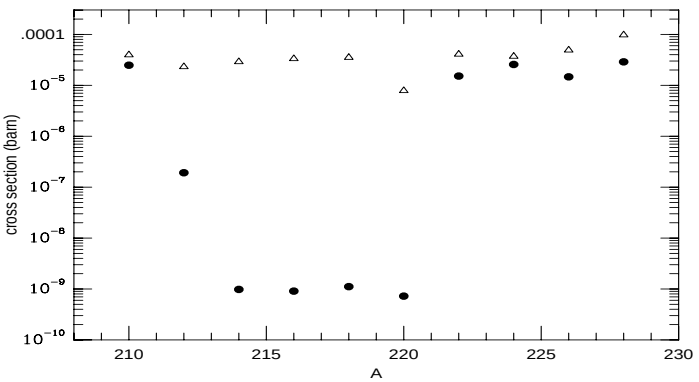

FIG. 1. 30 keV cross sections for different Pb isotopes. Levels and masses are calculated with models by Sharma et al. (8) (dots) and Möller et al. (9) (triangles).

comparison, the levels from both models are shown for ^{211}Pb and ^{215}Pb in Table 1. Only after the $1i_{11/2}$ shell (which forms the state at lowest energy in the RMFT) has been filled completely at ^{222}Pb the cross section is increasing because low spin states become available again.

The values resulting from the Möller model exhibit a smoother behavior. Only a slight dip is visible for ^{220}Pb(n,γ) since the previously accessible $1/2^+$ and $3/2^+$ states have become unbound in ^{221}Pb. Beyond ^{223}Pb the $2g_{9/2}$ shell (which is at lower energy than the $11/2^+$ level in this model) has been filled and at least one of the low spin states can be populated again. The known

TABLE 1. Comparison of theoretical bound energy levels (only the even parity states are shown)

^{211}Pb				^{215}Pb			
RMFT (8)		Möller (11)		RMFT (8)		Möller (11)	
E_x [MeV]	J^π	E_x [MeV]	J^π	E_x [MeV]	J^π	E_x [MeV]	J^π
0.000	11/2+	0.000	9/2+	0.000	11/2+	0.000	9/2+
1.317	9/2+	0.520	11/2+	1.479	9/2+	0.290	11/2+
3.139	5/2+	2.260	5/2+			1.224	5/2+
3.277	7/2+	3.218	1/2+			2.885	1/2+
3.327	1/2+	3.431	7/2+			3.029	7/2+

ground state spins for the lighter isotopes are also reproduced correctly.

If the r-process path crosses the Pb-isotopes in the masses range 212–220 due to the comparatively long β-decay half lives the sudden drop in the neutron capture cross section would terminate the r-process and prevent the build-up of heavier elements. Since in some cases there are unbound low spin states (J^π=1/2$^+$, 3/2$^+$) close to the threshold a small shift in the level energies could already close the gap. However, note that the level spacing in the RMFT has the tendency to increase towards neutron rich nuclei (13), contrary to the Möller prediction (and contrary to a recent Hartree-Fock calculation (14)).

Nevertheless, even if improved shell model descriptions and/or experiments have to clarify this point, the mechanism of cross section suppression due to the lack of low spin states could still be a possible restraint for the r-process path towards even more neutron rich isotopes and for nuclei beyond Pb. Because of the low level density the compound nucleus model would not be applicable in those cases.

V. ACKNOWLEDGEMENTS

We want to thank P. Möller and M.M. Sharma for making their computer codes available to us. This work was supported by the Austrian Science Foundation (project P8806–PHY). TR is an Alexander von Humboldt fellow.

REFERENCES

1. Balogh, W., Bieber, R., Oberhummer, H., Rauscher, T., Kratz, K.-L., Mohr, P., Staudt, G., and Sharma, M.M., in *Proc. Europ. Workshop on Heavy Element Nucleosynthesis*, eds. E. Somorjai and Z. Fülöp, Debrecen: Inst. Nucl. Res., 1994, p. 67.
2. Grün, K., Pichler, R., and Oberhummer, H., in *Proc. 4th Int. Conf. Appl. Nucl. Techn.*, in print.
3. Kim, K.H., Park, M.H., and Kim, B.T., *Phys. Rev. C* **23**, 363 (1987).
4. Krauss, H., computer code TEDCA, TU Wien, 1992, unpublished.
5. Kobos, A.M., Brown, B.A., Lindsay, R., and Satchler, G.R., *Nucl. Phys.* **A425**, 205 (1984).
6. Gambhir, Y.K., Ring, P., and Thimet, A., *Ann. Phys. (NY)* **198**, 132 (1990).
7. Sharma, M.M., Nagarajan, M.A., and Ring, P., *Phys. Lett. B* **312**, 377 (1993).
8. Sharma, M.M., Lalazissis, G.A., and Ring, P., *Phys. Lett. B* **317**, 9 (1993).
9. Möller, P. and Nix, J.R., *Nucl. Phys.* **A361**, 117 (1981).
10. Pradhan, H.C., Nogami, Y., and Law, J., *Nucl. Phys.* **A201**, 357 (1973).
11. Möller, P. and Randrup, J., *Nucl. Phys.* **A514**, 1 (1990).
12. Möller, P., Nix, J.R., Myers, W.D., and Swiatecky, W.J., *At. Data Nucl. Data Tables*, in print.
13. Sharma, M.M., Lalazissis, G.A., Hillebrandt, W., and Ring, P., *Phys. Rev. Lett.* **72**, 1431 (1994).
14. Dobaczewski, J., et al., *Phys. Rev. Lett.* **72**, 981 (1994).